

RSC Advances



This is an *Accepted Manuscript*, which has been through the Royal Society of Chemistry peer review process and has been accepted for publication.

Accepted Manuscripts are published online shortly after acceptance, before technical editing, formatting and proof reading. Using this free service, authors can make their results available to the community, in citable form, before we publish the edited article. This *Accepted Manuscript* will be replaced by the edited, formatted and paginated article as soon as this is available.

You can find more information about *Accepted Manuscripts* in the [Information for Authors](#).

Please note that technical editing may introduce minor changes to the text and/or graphics, which may alter content. The journal's standard [Terms & Conditions](#) and the [Ethical guidelines](#) still apply. In no event shall the Royal Society of Chemistry be held responsible for any errors or omissions in this *Accepted Manuscript* or any consequences arising from the use of any information it contains.

Enhanced Properties of Poly(vinyl alcohol) Composite Films with Functionalized Graphene

Shenbin Mo^a, Li Peng^b, Chunqiu Yuan^a, Chunyan Zhao^a, Wei Tang^a, Cunliang Ma^a, Jiaxin Shen^a, Wenbin Yang^b, Youhai Yu^{c*}, Yong Min^{a*} and Arthur J. Epstein^d

^a *Institute of Advanced Materials, Nanjing University of Posts and Telecommunications, 9 Wenyuan Road, Nanjing, Jiangsu 210046, China.*

^b *Yancheng Additive Manufacturing Technology Co., Ltd, 2 Xinyue Road China, Yancheng, Jiangsu 224005, China*

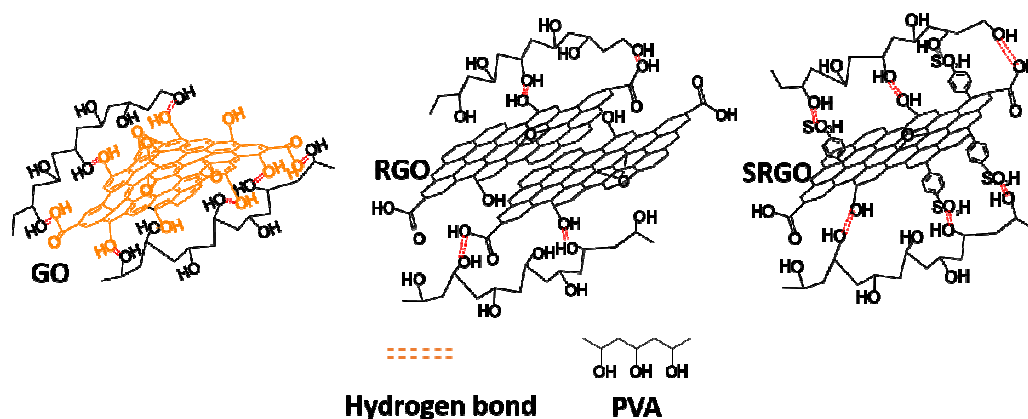
^c *Xi'an Institute of Optics and Precision Mechanics of Chinese Academy of Science, Xi'an 710119, China*

^d *Department of Physics and Chemistry & Biochemistry, The Ohio State University, 100 West 18th Avenue, Columbus, OH 43210, USA.*

Abstract

Three types of poly(vinyl alcohol) (PVA) composite films containing graphene oxide (GO), reduced graphene oxide (RGO) and a novel sulfonated graphene oxide (SRGO) as filler were successfully prepared by a simple solution casting. The structure and properties of graphene-based PVA composites films were investigated. Results showed that the properties of polymer composites films were sensitive to the structure of graphene. GO acted as the best reinforcing filler to enhance the mechanical property of PVA because it abounded with oxygen functional groups which could enhance the interfacial interactions through the formation of hydrogen bonds with PVA chains. The tensile strength and modulus of the resulting PVA/GO composites could reach 280 MPa and 13.5 GPa, respectively. RGO could improve the dielectric properties of PVA and the electrical conductivities were increased by $\sim 10^{11}$ orders of magnitude in the composites with 50 wt % of filler loadings as compared to that of neat PVA. SRGO could enhance the mechanical and dielectric properties of PVA simultaneously. The mechanical properties of PVA could be efficiently improved due to the strong interaction between the $-\text{SO}_3\text{H}$ groups on the SRGO sheets and PVA chains. The tensile strength and modulus of the resulting PVA/SRGO composites could reach 252 MPa and 8.5 GPa, respectively. Although the conductivity values of PVA/SRGO composites was less than that of that of PVA/RGO composites, it was still increased by $\sim 10^{10}$ orders of magnitude in the composites with 50 wt % of filler loadings as compared to that of neat PVA. These results demonstrated that PVA films with enhancement in mechanical and electronic properties can be fabricated with proper modified graphene.

Graphical abstract



Highlight

- . Three types of functionalized graphene, graphene oxide (GO), reduced graphene oxide (RGO) and a novel sulfonated graphene (SRGO) were prepared.
- . The poly(vinyl alcohol) (PVA) composites containing three types of functionalized graphene were successfully prepared by a simple solution casting.
- . The PVA/SRGO composite shows dramatic enhancements of both mechanical and dielectric properties of PVA.

Keywords

Functionalized graphene, sulfonated graphene, Poly(vinyl alcohol), Composite Films

1 Introduction

Graphene, a two-dimensional material consisting of a single layer of carbon atoms arranged in a honeycomb network, has attracted tremendous interest due to its high specific area and super-mechanical, electrical and thermal properties¹⁻⁴. Owing to these outstanding properties, graphene and its derivatives (graphene oxide (GO)/reduced graphene oxide (RGO), functionalized graphene, etc.) have been widely studied in various fields including energy devices⁵⁻⁹, conductive materials^{10,11}, drug delivery^{12,13} and polymer composites^{14,15}. In recent years, polymer/graphene composites have attracted a tremendous amount of attention to obtain high-performance light-weight materials. To achieve maximal properties enhancement, the manufacturing of such composites requires that the graphene is dispersed homogeneously in the matrix and the external load is efficiently transferred via a strong interaction at the interface between the graphene and the matrix. However, the homogeneous dispersion of graphene in the polymer matrix remains challenging due to the scarcity of a soluble/dispersible graphene in a common solvent with the polymer. So far GO is mostly used to make the polymer composites, which can undergo exfoliation completely in water, dimethyl-sulfoxide (DMSO) and dimethylformamide (DMF). It is possible to achieve a truly molecular-level

dispersion of graphene oxide in the polymer matrix if the solvent could dissolve the polymer matrix. On the other hand, graphene oxide (GO) contains many oxygen functional groups, such as hydroxyls, epoxides, carboxyls and carbonyls, which can improve the dispersion and form strong hydrogen bonds with polymer molecules. But the intrinsic conductive and mechanical properties of GO are much lower than those of graphene/reduced graphene oxide (RGO) ¹⁶⁻¹⁸. It has been demonstrated that the high performance of polymer composites not only depends on optimizing the dispersion and interface load transfer, but also depends on the intrinsic properties of the filler ^{19, 20}. In fact, many effects have already tried improving the intrinsic properties of the filler by in situ chemical reduction of GO mixed with polymer matrices ^{21,22}. However, the electrical properties of the RGO /polymer composites can be improved with the loss of mechanical properties. After reduction of GO to RGO, the structure of graphene is partly restored, which inevitably results in a significant decrease in the oxygen functional groups of RGO and then poor interfacial interactions between RGO sheets and polymer matrices. Reduced interfacial interactions would weaken the reinforcing effect of increased intrinsic mechanical strength of RGO ^{20,23}.

To solve these problems, we proposed to use the $-SO_3H$ group functionalized RGO (SRGO) to make the polymer composites. The SRGO may form stable dispersion in polar solvents and exhibited good electrical conductivity ²⁴. Thus, functionalized graphene/polymer composites with increased both the conductivity and mechanical properties maybe yield. We selected poly(vinyl alcohol) (PVA), a hydroxyl-rich, water-soluble polymer, as a model polymer matrix, which forms hydrogen bonds with $-SO_3H$ group anchored on SRGO easily. Therefore, it is anticipated that the chemically functionalized graphene sheets interact well with the PVA matrices, resulting in percolation of mechanical and electrical properties of the composites. We fabricated three different types of poly(vinyl alcohol) (PVA) composite films containing GO, RGO and SRGO as nanofiller by a simple solution casting. The properties and structures of PVA/ graphene nanocomposites were extensively investigated, which enable us to better understand the structure–property relationships in polymer composites.

2 Experimental

2.1 Materials.

Chemicals and materials

Graphite powder was purchased from Baichuan Graphite Ltd. (Qingdao, China). Concentrated H_2SO_4 (98 %), HCl (36%), $KMnO_4$, H_2O_2 (30%) solution, sodium borohydride, sulfanilic acid and sodium nitrate were purchased from Sinopharm Chemical Reagent Co., Ltd. (Shanghai, China). Borofluoride was purchased from SSS Reagent Co., Ltd. (Shanghai, China). PVA was purchased from Sigma-Aldrich. Unless otherwise specified, all reagents were used without further purification.

2.2 Synthesis

2.2.1 Preparation of GO, RGO and SRGO

GO was prepared from natural flaked graphite according to a modified pressurized oxidation²⁵. Briefly, a solution of 5.0 g of graphite and 200 mL H₂SO₄ (98%) was stirred in ice bath for 30 min, 18.0 g K₂MnO₄ was slowly added with stirring for 30 min. The solution was heated to 35 °C for 2 h, then added slowly into 1600 mL of deionizer water. After cooling down, 10 mL H₂O₂ (30%) was added to give an orange yellow solution. The precipitate was centrifuged and then washed successively with 1 M HCl solution and deionized water. Finally, powdered GO was obtained by lyophilizing at -48 °C, 18 Pa.

RGO was obtained by the following process: 1g of GO is dispersed in 500 ml water and sonicated for 30 mins. Then 1.5g sodium borohydride was added into GO dispersion and kept at 80 °C under constant stirring. After 30mins, another 3.3g sodium borohydride was added and kept stirring for 1 h. The product was centrifuged and washed with water thoroughly. Finally, RGO was obtained by lyophilizing at -48 °C, 18 Pa.

SRGO was prepared by the sulfonation of RGO with diazonium salt of sulfanilic acid²⁴. For this purpose, the aryl diazonium salt of sulfanilic acid was prepared first. 35.2g sulfanilic acid was dissolved in 100 ml water in the ice bath and 86ml HBF₄ was added slowly under constant stirring for 30mins. Then 15.2g sodium nitrate was added and kept stirring for 1h. The product, diazonium salt of sulfanilic acid, was filtered and washed with ethanol thoroughly. For diazonium coupling, 1g RGO was dispersed in 500ml water, then the resulting diazonium salt of sulfanilic acid was added at 0°C and was kept for 2h with stirring. The mixture was centrifuged, washed with water thoroughly, and lyophilized to give SRGO.

2.2.2 Composite preparation

PVA/SRGO composites with different amounts of SRGO loadings varying from 10 to 50 wt % were synthesized by a simple solution casting. 0.2 g of PVA was dissolved in 50 ml hot distilled water then the desired amount of SRGO dispersion (10, 20, 30, 40 and 50 wt % with respect to the PVA/SRGO composite) was slowly added into the PVA solution. The resulting mixture was stirred for 30mins to form a homogeneous solution. Subsequently, the obtained homogeneous solution was slowly casted onto a plate and dried at 60°C to form a flat film. Finally, the film was peeled off. In order to compare the improvement in physical properties of PVA/SRGO composites, a series of PVA/GO and PVA/RGO films with different amounts of GO and RGO loadings were fabricated in similar way, respectively.

2.3 Characterizations

X-ray photoelectron spectroscopy (XPS) analysis was conducted on a PHI 5000 VersaProbe analyzer (UIVAC-PHI Ltd.) using focused monochromatized Al Ka radiation (1486.6eV) generated at 15 kV. Fourier transform infrared spectrometer (FTIR) of the samples were recorded with an IR Prestige-21 FT-IR spectrometer. X-ray diffraction (XRD) were performed with an X'Pert Pro (PANalytical) diffractometer using monochromatic Cu K α 1 radiation ($\lambda = 1.5406 \text{ \AA}$) at 40 kV. The morphology of as-prepared samples was characterized by a scanning electron microscope (SEM, Hitachi S-4800 field emission). The samples were fractured in

liquid nitrogen and coated with a thin layer of gold prior to observations. Transmission electron microscopy (TEM) was conducted using HITACHI HT7700 with an accelerating voltage of 100 KV. Thin films of PVA/GO, PVA/RGO and PVA/SRGO composite solution were subjected to ultrasonication treatment and then casted onto the carbon-coated copper grid, which was dried at room temperature before TEM analysis.

The tensile experiments were carried out on a universal testing machine (Zhuhai SUST Electrical Equipment Co., Ltd., China, model CMT4304) at a strain rate of 5mm/min. The reported values were calculated as averages over 5 specimens for each group of specimens.

The electrical conductivity was measured with a ST2258A high resistance meter (Suzhou Jingge Electronic Co., Ltd, China). Five parallel runs were done in the case of each sample and the average was reported.

3. Results and discussion

3.1 characterization of samples

The elemental compositions of GO, RGO, and SRGO were investigated via XPS analysis. Fig. 1A shows XPS surveys of GO, RGO, and SRGO. The obvious S 2p peak appeared at 167 eV in SRGO, indicating the successful sulfonation of graphene sheets. The C1s signals contributed by the C=O C-O and C-OH groups are significantly decreased in RGO and SRGO suggesting that most of the oxygen functionalities were removed from the surfaces of RGO and SRGO compared to GO. (Fig. 1B, C and D) All of these observations suggest that the grafting of $-\text{SO}_3\text{H}$ group on the graphene sheets and its existence does not affect the reduction of GO on the surface of graphene sheet.

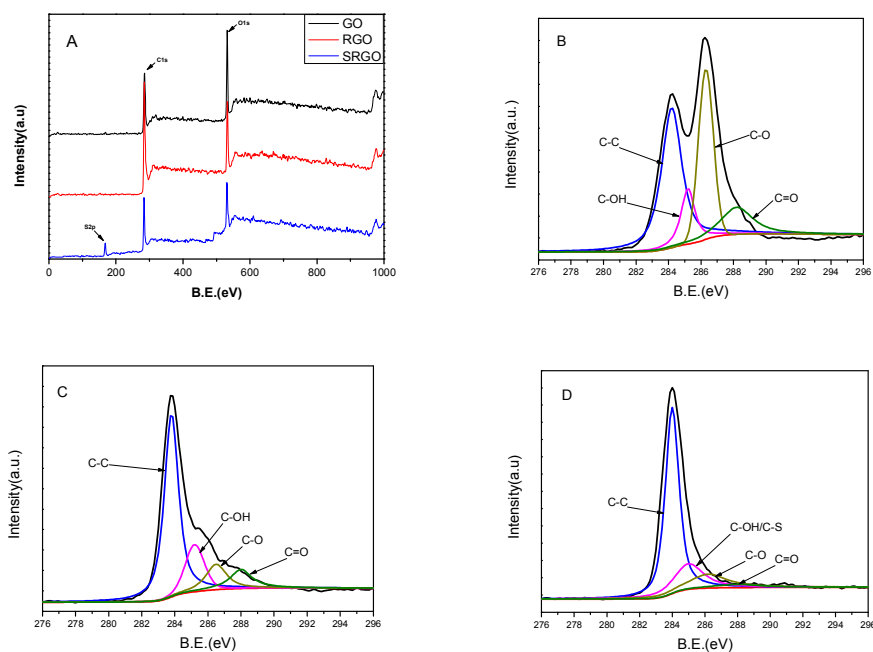


Figure 1. (A) XPS survey of GO, RGO and SRGO; C1s XPS data of (B) GO, (C) RGO, and (D) SRGO.

The digital images of the GO, RGO and SRGO dispersed in water are shown in Fig. 2A. GO sheets can be dispersed well in water due to their oxygen-containing functional groups. After reducing, the color of GO suspension changes from brownish-yellow to black, indicating the efficient reduction of GO. However, the RGO sheets form irreversible hydrophobic agglomerates and lose its water dispersibility due to the removal of the oxygen-containing groups. For SRGO, the presence of hydrophilic functional groups of $-\text{SO}_3\text{H}$ attached to the surface of graphene facilitated to form stable water dispersion. The PVA/GO composite film was brownish-yellow (Fig. 2B-1), while the PVA/RGO and PVA/SRGO composite films were black, as shown in Fig. 2B-2 and Fig. 2B-3. The dispersion qualities of GO, RGO and SRGO in PVA matrix were further analyzed with TEM. The PVA/GO, PVA/RGO and PVA/SRGO exhibited different morphological behavior, as shown in Fig. C-E. Many linear wrinkles across the surface of GO were observed in PVA/GO composites, which is a common feature of GO attributed to the defects caused by oxidation²⁶. GO disperse quite well in the PVA matrix, and no obvious agglomerate was observed. On the other hand, RGO and SRGO displayed relatively smooth surface in the PVA matrix, suggesting that most of the oxygen functionalities were removed from their surfaces. The sizes of SRGO sheets were smaller than that of RGO sheets, which is caused by sulfonating treatment. The agglomeration of RGO or SRGO sheets can be observed in the PVA matrix. ,

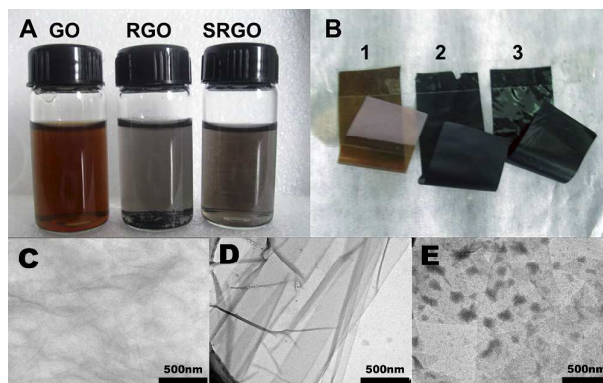


Figure 2. A: Digital images of aqueous suspensions of GO, RGO and SRGO. B: Digital images of PVA composite films filled with 30 wt % of: (1) GO, (2) RGO and (3)SRGO. TEM images of PVA composite films filled with 30 wt% of: (C) GO, (D) RGO and (E)SRGO

SEM micrographs were taken to examine the fracture surface morphologies of PVA composite films. The fracture surface morphologies of pure PVA and graphene film materials were also studied to compare with PVA composites. Graphene film materials were fabricated by vacuum-assisted filtration of the aqueous dispersions of RO, ROG and SRGO. The neat PVA fracture surface exhibits a relatively smooth surface, as shown in Fig. 3A and Fig. 3B. SEM images of the fracture surfaces of the GO and RGO material (Fig. 3C and Fig. 3E) show typical laminated morphology of graphene papers, consisted of GO or RGO flakes well-aligned in the plane of the paper. The RGO flakes are more compacted compared with GO flakes due to the

strong π - π interaction between RGO sheets. The fracture surfaces of the SRGO material also appears to be stratified, but the flakes are much less well defined and the stack is much loose. The fracture surfaces of PVA composites are remarkably different from that of neat PVA and graphene materials. They are rougher than that of PVA, but smoother than that of graphene materials. This is exactly what it would be expected if graphene materials were covered with a PVA polymer coating. The fracture surface of the PVA/GO composite (Fig. 3C and Fig. 3D) and that of PVA/SRGO composite (Fig. 3E and Fig. 3F) are both layer structured, although they are not well-ordered. The fracture surfaces of PVA/RGO (Fig. 3G and Fig. 3H), on the other hand, show a well-ordered layered structure. In the meantime, the roughness of the fracture surface significantly increases compared with that of PVA/GO and PVA/SRGO and the surface of RGO sheets could be clearly exposed during the process of freeze fracture. These results provide the evidence that both GO and SRGO have stronger interfacial interaction with PVA matrix than RGO does.

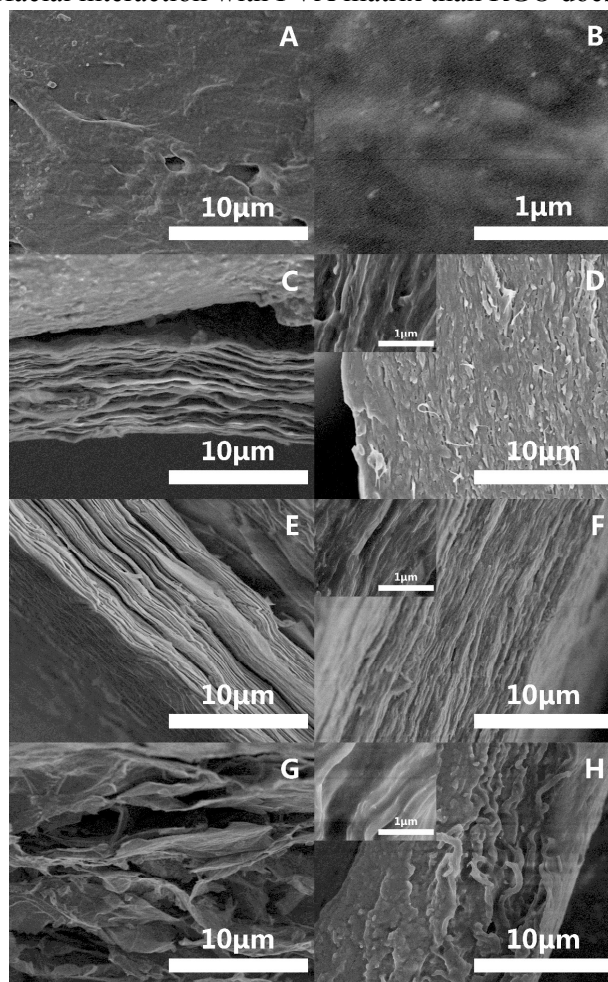


Figure 3 SEM images of the fracture of PVA (A,B), and PVA composite films filled with 30 wt% of: (C,D) GO, (E,F) RGO and (G,H)SRGO

XRD patterns of GO, RGO, SRGO, PVA and their composites are shown in Fig. 4. An intense peak centered at $2\theta = 10.56$ can be observed in the XRD pattern of GO, which

is corresponding to an average interlayer spacing of 0.84 nm. At the same time, and the basal reflection (002) peak at $2\theta = 26.5$ (d spacing = 0.34 nm) of pristine graphite disappears in GO²⁷. The interlayer spacing of GO is increased from 0.34 to 0.84 nm due to the intercalation of oxygen-containing functional groups and water molecules in-between the graphite layers²⁸. For RGO, the peak at $2\theta = 10.56$ shifts to 26.0, suggesting the removal of interlayer oxygen functional groups and the formation of a multilayer stack of graphene due to the π - π interaction. Similarly, SRGO exhibits a very broad hump centered at $2\theta = 26$ due to the formation of a few layer functionalized graphene. This broad hump also indicates the poor ordering of the sheets along the stacking direction. Pure PVA shows a diffraction peak at $2\theta = 19.4$, consistent with the literature^{29, 30}. The PVA/GO composites, as shown in Fig. 4B, only exhibit peaks close to that of neat PVA with no characteristic peak of GO. This result implies that GO sheets were fully exfoliated and dispersed homogeneously in the PVA matrix,³¹ which is in line with the TEM results.

However, in the case of PVA/RGO and PVA/SRGO composites (Fig. 4C and Fig. 4D), they all show two broad diffraction, which can be attributed to PVA and RGO/SRGO layers respectively. Unlike GO which can be easily dispersed well in aqueous media due to its abundance surface oxygen groups, RGO/SRGO may agglomerate in water because of the strong π - π interaction between sheets. Thus, a multiple layers of RGO /SRGO formed in the PVA matrix. We also noted that the intensity of the diffraction peaks belong to PVA in all of composites is weaker than that of neat PVA, showing a decrease in crystallinity and indicating that some interactions between the polymer chains and filler may take place^{22, 32}.

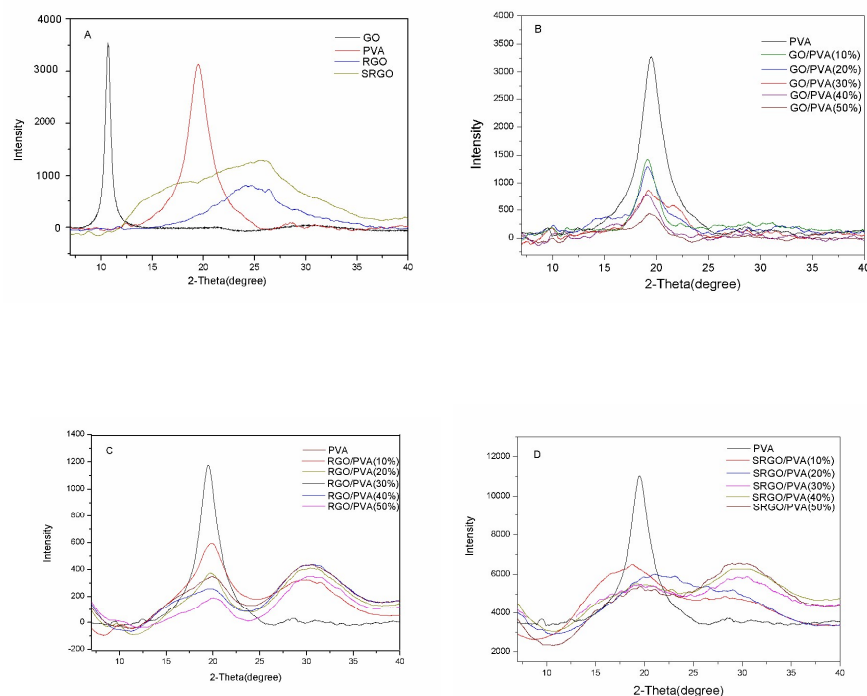


Figure 4. XRD patterns of (A) GO, RGO, SRGO, PVA and (B, C, D) PVA composites

with various types and amounts of filler.

The FT-IR spectra were recorded to characterize GO, RGO, SRGO, PVA, PVA/SRGO, PVA/RGO, and PVA/GO composites are shown in Fig. 5. The spectrum of GO illustrates the presence of C-O (ν C-O at 1065cm^{-1}), C-O-C (ν C-O-C at 1240cm^{-1}), C-OH (ν C-OH at 1390cm^{-1}), and C-O in carboxylic acid and carbonyl moieties (ν C=O at 1730cm^{-1}). The peak at 1620cm^{-1} may be from skeletal vibrations of unoxidized graphitic domains. In the spectrum of RGO and SRGO, the intensities of the bands associated with the oxygen functional groups decrease significantly or even disappear, indicating the deoxygenation of GO upon reduction. In comparison to GO and RGO, the distinguished features of SRGO is the presence of some new absorptions as a result of successful SO_3H groups modification. The peaks at 1175cm^{-1} , 1126cm^{-1} , and 1040cm^{-1} (two ν S-O and one ν s-phenyl) confirm the presence of a sulfonic acid group, and the peaks at 1007cm^{-1} (ν C-H in-plane bending) and 830cm^{-1} (out-of-plane hydrogen wagging) are characteristic vibrations of a *p*-disubstituted phenyl group²⁴. In the spectrum of PVA, the appearance of a broad peak at 3300cm^{-1} is attributed to the symmetrical stretching vibration of hydroxyl groups, and the band at 1080cm^{-1} corresponds to the stretching vibration of the epoxide groups in PVA²⁰. The hydroxyl peaks in the PVA/SRGO, PVA/RGO, and PVA/GO composites are shifted to smaller wavenumbers compared with pure PVA due to the formation of a hydrogen bonds between the hydroxyl groups of PVA and functionalized graphene^{21, 32}.

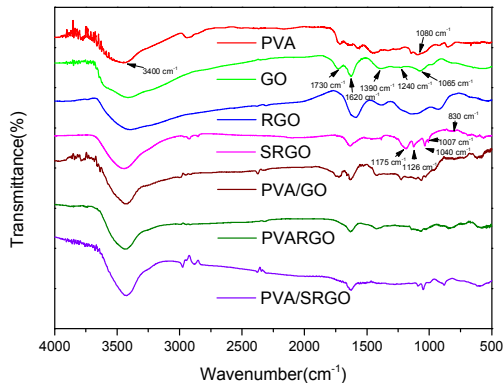


Figure 5. FITR for GO, RGO, SRGO, PVA and PVA composite films filled with 30 wt % of GO, RGO and SRGO

3.2 Mechanical properties

Fig. 6A-C shows the representative stress-strain curves of PVA composites with various amounts of GO, RGO and SRGO loading. Table 1 summarizes the mechanical properties of different PVA composites. In all cases of PVA composites, tensile strength and modulus improve significantly compared to the neat PVA. Both GO/PVA and SRGO/PVA are mechanically robust, and the tensile strength and modulus values

varie widely with the changes in the GO or SRGO content. Specifically, the GO/PVA composites containing 10 wt.% of GO have the average tensile strength of 195 ± 15 MPa, and it continuously increased up to 280 ± 18 MPa with 30 wt.% of GO loading. At the same time, the tensile modulus improved from 5.3 ± 0.9 to 13.5 ± 1.2 GPa. However, further increase of the content of GO will decrease the mechanical properties. For the GO/PVA composites containing 50 wt % of GO, the tensile strength and modulus value is 213 ± 14 MPa and 11.4 ± 0.7 , respectively. This trend is also observed in the SRGO/PVA composites. For SRGO/PVA composites, the best tensile strength value is 252 ± 25 MPa with modulus value as 8.5 ± 1.8 belongs to the composites with 40 wt % of SRGO. The tensile strength values of the RGO/PVA composites are much lower than those of GO/PVA and SRGO/PVA composite, and slightly affected by the changes in filler content. The tensile strength of the RGO/PVA composite continuously decreased from 83.2 MPa to 51.3 MPa, with the content of RGO increased from 10wt% to 50wt%.

There are probably two factors to influence the mechanical properties of PVA composites: Hydrogen bonds between the fillers and PVA matrix and mechanical strength of fillers²⁰. For GO/PVA composite, the improved mechanical properties with the amount of the filler increasing may be explained as it significantly reinforced the hydrogen bonding network of PVA-based composites and increased mechanical strength from GO sheets. However, further increase of the content of GO will decrease the mechanical properties due to the agglomeration of GO, which will reduce the amount of oxygen-containing functional groups on the surface of GO sheets and weak the hydrogen bonding network with PVA. Our TEM results show that unlike GO dispersed well in PVA matrix, RGO and SRGO tend to agglomerate in PVA matrix because of the strong π - π interaction between sheets. Since interfacial interaction is dependent on the surface area, a decrease in interfacial interaction is expected in aggregated state. However, our SRGO/PVA composites show equivalent mechanical properties as GO/PVA composites. This may be attributed to the $-\text{SO}_3\text{H}$ groups on the SRGO sheets, which will interact much stronger with PVA than the $-\text{COOH}$ groups on GO and better mechanical strength of SRGO sheets³³. In the case of RGO, given the much less presence of oxygen-containing functional groups on the surface of RGO sheets, the interaction between PVA and RGO via hydrogen bonding should be much weaker. The improved mechanical properties in the PVA/RGO composite compared with neat PVA mainly come from the mechanical strength of RGO layers. The elongation at breaks for all three types of composite decreased in composites with filler loadings, suggesting increased stiffness with graphene loadings compared to the neat polymer. This is attributed to the interfacial adhesion between the filler and PVA matrix by the formation of hydrogen bonds with the hydroxyl functionalities. This kind of bond formation restricts the mobility of the PVA chain segment and consequently decreases the strain of the composites³⁴.

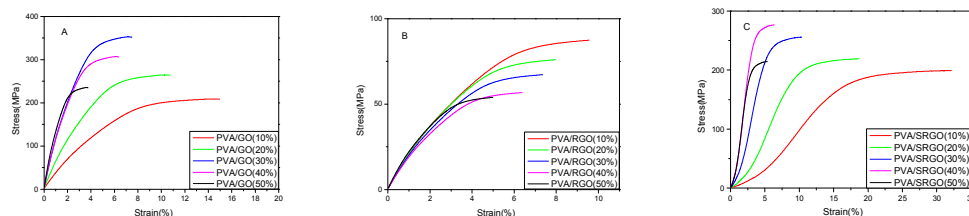


Figure 6. Stress–strain curves of (A) PVA/GO, (B) PVA/RGO and (C) PVA/SRGO composites with various amounts of filler loading

Table 1

Tensile properties of pure PVA and its composites with GO, RGO and SRGO.

Sample	Tensile strength (MPa)	Tensile modulus (GPa)	Elongation at break (%)
PVA	50±1.4	2.3±0.1	73.2±1.3
PVA/GO-10 wt. %	195±15	5.3±0.9	13.7±2.3
PVA/GO-20 wt. %	233±20	8.7±1.0	11.5±1.8
PVA/GO-30 wt. %	280±18	13.5±1.2	7.7±2.3
PVA/GO-40 wt. %	243±13	12.5±1.5	5.8±1.9
PVA/GO-50 wt. %	213±14	11.4±0.7	4.2±1.2
PVA/RGO-10 wt. %	83.2±2.1	2.8±0.5	13.2±2.1
PVA/RGO-20 wt. %	75.2±2.7	3.0±0.3	10.1±1.9
PVA/RGO-30 wt. %	65.7±3.2	3.2±0.6	7.6±2.0
PVA/RGO-40 wt. %	58.7±5.1	4.5±1.0	4.3±1.5
PVA/RGO-50 wt. %	51.3±2.4	4.8±0.7	2.3±1.1
PVA/SRGO-10 wt. %	193±18	3.7±1.2	28.7±5.7
PVA/SRGO-20 wt. %	210±15	4.7±1.1	20.3±3.8
PVA/SRGO-30 wt. %	235±20	6.5±1.2	13.8±2.5
PVA/SRGO-40 wt. %	252±25	8.5±1.8	10.4±3.6
PVA/SRGO-50 wt. %	215±18	9.8±1.7	5.4±2.5

3.3 Electrical conductivity

Graphene is a good conductor of electricity and PVA is an insulator ($\sigma = 5.3 \times 10^{-14}$ S/cm). The PVA/graphene composites were expected to exhibit good electrical conductivity due to the exceptionally high conductivity of graphene. Thus the electrical conductivity of PVA nanocomposites is investigated. The volume electrical conductivities of nanocomposite membranes were measured and plotted in Fig. 7. For PVA/RGO and PVA/SRGO composites, the log of the electrical conductivity increased as the filler contents increased, indicating the improvement of electrical conductivity. The PVA/SRGO composites show lower electrical conductivity compared to PVA/RGO composites, indicating that the RGO sheets could more efficiently improve the electrical conductivity of nanocomposites than SRGO sheets. This is due to the adsorption of insulating $-\text{SO}_3\text{H}$ on the surface of SRGO sheets²⁴. In the case of GO, the charge conducting structure is destructed due to the disrupted conjugation and lattice defects caused by oxygenation, so PVA/GO nanocomposites

have much poorer electrical conductivity. All these findings suggest that the high electrical conductivity of RGO and SRGO is useful in the fabrication of conductive polymer composites for different applications.

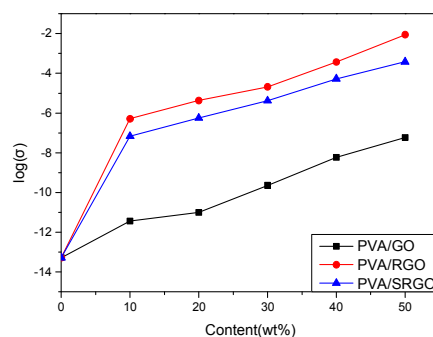


Figure 7 Electrical conductivity (σ) of PVA/GO, PVA/RGO, and PVA/SRGO with different filler loading.

4 Conclusions

Three types of functionalized graphene, graphene oxide (GO), reduced graphene oxide (RGO) and a novel sulfonated graphene oxide (SRGO) were synthesized using graphite as starting material. They were then successfully incorporated into the PVA matrix as evidenced by XPS, SEM, XRD and FT-IR analysis. The properties of the resulting PVA composite films are sensitive to the structures of fillers. The PVA/GO composite films exhibited a remarkable enhancement in mechanical properties due to GO can form strong hydrogen bonds with the PVA matrix and achieved good dispersion in the PVA matrix. When GO is reduced, the oxygen functional groups of RGO significantly decrease, and the electrical conductivity was increased by 5 orders in PVA/RGO composite films. However, the poor interfacial interactions between RGO sheets and PVA chains lead to a limited improvement of mechanical properties of PVA/RGO nanocomposite films. SRGO was obtained by anchoring $-\text{SO}_3\text{H}$ group on the RGO surface, and PVA/SRGO obtained remarkable enhancements in both mechanical properties and electrical conductivity. The stronger H-bonding between the $-\text{SO}_3\text{H}$ group in SRGO and the $-\text{OH}$ group of PVA, as well as the larger mechanical strength of SRGO sheets compared with GO are reasons for the increased mechanical properties. The conductivity values of PVA/SRGO did not differ significantly from that of PVA/RGO due to the formation of a conducting network in the PVA matrix. These findings suggest that polymer films with enhancement properties can be fabricated by choosing proper functionalized graphene as filler.

Acknowledgements

The authors would like to acknowledge the financial support by Nanjing University of Posts and Telecommunications basic research program (NY 212002), the Ministry of Education of China Innovative Research Team in University (IRT1148) and the Key

Project of National High Technology Research of China (2011AA050526).

Reference

1. K. S. Novoselov, A. K. Geim, S. V. Morozov, D. Jiang, Y. Zhang, S. V. Dubonos, I. V. Grigorieva and A. A. Firsov, *Science*, 2004, **306**, 666-669.
2. A. K. Geim, *Science*, 2009, **324**, 1530-1534.
3. C. Lee, X. Wei, J. W. Kysar and J. Hone, *Science*, 2008, **321**, 385-388.
4. A. A. Balandin, S. Ghosh, W. Bao, I. Calizo, D. Teweldebrhan, F. Miao and C. N. Lau, *Nano Lett.*, 2008, **8**, 902-907.
5. M. Liang and L. Zhi, *Journal of Materials Chemistry*, 2009, **19**, 5871-5878.
6. F.-Y. Su, C. You, Y.-B. He, W. Lv, W. Cui, F. Jin, B. Li, Q.-H. Yang and F. Kang, *Journal of Materials Chemistry*, 2010, **20**, 9644-9650.
7. L. Valentini, M. Cardinali, S. B. Bon, D. Bagnis, R. Verdejo, M. Angel Lopez-Manchado and J. M. Kenny, *Journal of Materials Chemistry*, 2010, **20**, 995-1000.
8. W. Tang, L. Peng, C. Yuan, J. Wang, S. Mo, C. Zhao, Y. Yu, Y. Min and A. J. Epstein, *Synthetic Metals*, 2015, **202**, 140-146.
9. J. Yan, J. Liu, Z. Fan, T. Wei and L. Zhang, *Carbon*, 2012, **50**, 2179-2188.
10. J. Geng, L. Liu, S. B. Yang, S.-C. Youn, D. W. Kim, J.-S. Lee, J.-K. Choi and H.-T. Jung, *Journal of Physical Chemistry C*, 2010, **114**, 14433-14440.
11. J. Zhao, S. Pei, W. Ren, L. Gao and H.-M. Cheng, *Acs Nano*, 2010, **4**, 5245-5252.
12. X. Yang, X. Zhang, Y. Ma, Y. Huang, Y. Wang and Y. Chen, *Journal of Materials Chemistry*, 2009, **19**, 2710-2714.
13. R. Zhang, M. Hummelgard, G. Lv and H. Olin, *Carbon*, 2011, **49**, 1126-1132.
14. R. Verdejo, M. M. Bernal, L. J. Romasanta and M. A. Lopez-Manchado, *Journal of Materials Chemistry*, 2011, **21**, 3301-3310.
15. D. Cai and M. Song, *Journal of Materials Chemistry*, 2010, **20**, 7906-7915.
16. Y. Li, R. Umer, Y. A. Samad, L. Zheng and K. Liao, *Carbon*, 2013, **55**, 321-327.
17. C. Gomez-Navarro, M. Burghard and K. Kern, *Nano Lett.*, 2008, **8**, 2045-2049.
18. Y. Zhu, S. Murali, W. Cai, X. Li, J. W. Suk, J. R. Potts and R. S. Ruoff, *Advanced Materials*, 2010, **22**, 3906-3924.
19. T. Ramanathan, A. A. Abdala, S. Stankovich, D. A. Dikin, M. Herrera-Alonso, R. D. Piner, D. H. Adamson, H. C. Schniepp, X. Chen, R. S. Ruoff, S. T. Nguyen, I. A. Aksay, R. K. Prud'homme and L. C. Brinson, *Nature Nanotechnology*, 2008, **3**, 327-331.
20. C. Bao, Y. Guo, L. Song and Y. Hu, *Journal of Materials Chemistry*, 2011, **21**, 13942-13950.
21. H. Javier Salavagione, G. Martinez and M. A. Gomez, *Journal of Materials Chemistry*, 2009, **19**, 5027-5032.
22. X. Zhao, Q. Zhang, D. Chen and P. Lu, *Macromolecules*, 2010, **43**, 2357-2363.
23. L. Shao, J. Li, Y. Zhang, S. Gong, H. Zhang and Y. Wang, *Journal of Materials Chemistry A*, 2014, **2**, 14173-14180.
24. Y. Si and E. T. Samulski, *Nano Lett.*, 2008, **8**, 1679-1682.
25. C. Bao, L. Song, W. Xing, B. Yuan, C. A. Wilkie, J. Huang, Y. Guo and Y. Hu, *Journal of Materials Chemistry*, 2012, **22**, 6088-6096.
26. H. C. Schniepp, J. L. Li, M. J. McAllister, H. Sai, M. Herrera-Alonso, D. H. Adamson, R. K. Prud'homme, R. Car, D. A. Saville and I. A. Aksay, *Journal of Physical Chemistry B*, 2006, **110**,

- 8535-8539.
27. I. K. Moon, J. Lee, R. S. Ruoff and H. Lee, *Nature Communications*, 2010, **1**.
 28. T. Kuila, S. Bose, P. Khanra, A. K. Mishra, N. H. Kim and J. H. Lee, *Carbon*, 2012, **50**, 914-921.
 29. X. Yang, L. Li, S. Shang and X.-m. Tao, *Polymer*, 2010, **51**, 3431-3435.
 30. J.-H. Yang and Y.-D. Lee, *Journal of Materials Chemistry*, 2012, **22**, 8512-8517.
 31. Y. Xu, W. Hong, H. Bai, C. Li and G. Shi, *Carbon*, 2009, **47**, 3538-3543.
 32. L. Jiang, X.-P. Shen, J.-L. Wu and K.-C. Shen, *Journal of Applied Polymer Science*, 2010, **118**, 275-279.
 33. R. K. Layek, S. Samanta and A. K. Nandi, *Carbon*, 2012, **50**, 815-827.
 34. X. Wang, H. Bai, Z. Yao, A. Liu and G. Shi, *Journal of Materials Chemistry*, 2010, **20**, 9032-9036.